The EMBO Journal (2008) 27, 2214–2221 | © 2008 European Molecular Biology Organization | All Rights Reserved 0261-4189/08
www.embojournal.org

THE EMBO JOURNAL

Arabidopsis MAP kinase 4 regulates gene expression through transcription factor release in the nucleus

Jin-Long Qiu[1,6], Berthe Katrine Fiil[1,6], Klaus Petersen[1], Henrik Bjørn Nielsen[2], Christopher J Botanga[3], Stephan Thorgrimsen[1], Kristoffer Palma[1], Maria Cristina Suarez-Rodriguez[1], Signe Sandbech-Clausen[1], Jacek Lichota[4], Peter Brodersen[5], Klaus D Grasser[4], Ole Mattsson[1], Jane Glazebrook[3], John Mundy[1] and Morten Petersen[1,*]

[1]Department of Biology, University of Copenhagen, Copenhagen, Denmark, [2]Center for Biological Sequence Analysis, Department of Systems Biology, Technical University of Denmark, Kongens Lyngby, Denmark, [3]Department of Plant Biology and Center for Microbial and Plant Genomics, University of Minnesota, St Paul, MN, USA, [4]Department of Life Sciences, Aalborg University, Aalborg, Denmark and [5]Institut de Biologie Moléculaire des Plantes du CNRS, Unité Propre de Recherche 2357, 12 rue du Général Zimmer, Strasbourg Cedex, France

Plant and animal perception of microbes through pathogen surveillance proteins leads to MAP kinase signalling and the expression of defence genes. However, little is known about how plant MAP kinases regulate specific gene expression. We report that, in the absence of pathogens, *Arabidopsis* MAP kinase 4 (MPK4) exists in nuclear complexes with the WRKY33 transcription factor. This complex depends on the MPK4 substrate MKS1. Challenge with *Pseudomonas syringae* or flagellin leads to the activation of MPK4 and phosphorylation of MKS1. Subsequently, complexes with MKS1 and WRKY33 are released from MPK4, and WRKY33 targets the promoter of *PHYTOALEXIN DEFICIENT3* (*PAD3*) encoding an enzyme required for the synthesis of antimicrobial camalexin. Hence, *wrky33* mutants are impaired in the accumulation of *PAD3* mRNA and camalexin production upon infection. That WRKY33 is an effector of MPK4 is further supported by the suppression of *PAD3* expression in *mpk4–wrky33* double mutant backgrounds. Our data establish direct links between MPK4 and innate immunity and provide an example of how a plant MAP kinase can regulate gene expression by releasing transcription factors in the nucleus upon activation.

The EMBO Journal (2008) **27,** 2214–2221. doi:10.1038/emboj.2008.147; Published online 24 July 2008
Subject Categories: signal transduction; plant biology
Keywords: *Arabidopsis*; defence response; MAP kinase; target genes; transcription factor

*Corresponding author. Department of Biology, University of Copenhagen, Ole Maaloees Vej 5, Copenhagen 2200, Denmark. Tel.: +45 35322127; Fax: +45 35322128; E-mail: shutko@bio.ku.dk
[6]These authors contributed equally to this work

Received: 4 March 2008; accepted: 4 July 2008; published online: 24 July 2008

Introduction

Plants have evolved a multi-layered system of defence responses that can be activated upon recognition of invading pathogens. One layer includes transmembrane receptors that recognize evolutionarily conserved pathogen-associated molecular patterns (PAMPs) and when activated trigger an immune response. Successful pathogens can deliver effectors that suppress the immune response and contribute to pathogen virulence (Jones and Dangl, 2006). Another layer involves recognition of pathogen effector molecules through host resistance (*R*) genes, triggering a rapid defence response that often includes a localized programmed cell death reaction known as the hypersensitive response (Nimchuk *et al*, 2003).

Recognition by animal and plant innate immune systems activates defence responses mediated by protein kinase signalling pathways (DeYoung and Innes, 2006). These pathways regulate the expression of numerous genes, including genes involved in the production of antimicrobial compounds (Fehlbaum *et al*, 1994; Schonwetter *et al*, 1995; Zhou *et al*, 1999; Couillault *et al*, 2004). For example, the expression of some antimicrobial genes in mammals and *Drosophila* requires members of the NF-kappaB class of transcription factors (Meng *et al*, 1999; Diamond *et al*, 2000). Studies on *Arabidopsis* and other plants implicate MAP kinases and WRKY transcription factors in the regulation of genes required for pathogen resistance (Eulgem *et al*, 2000; Asai *et al*, 2002; Andreasson *et al*, 2005; Journot-Catalino *et al*, 2006; Xu *et al*, 2006). The genome of the model plant *Arabidopsis* encodes more than 20 MAP kinases, including MPK3, MPK4 and MPK6 implicated in innate immunity responses (Petersen *et al*, 2000; Asai *et al*, 2002; Menke *et al*, 2004). WRKY proteins constitute a large family of transcription factors in plants. They bind W-box sequences in the promoters of pathogen-induced genes, including WRKY genes themselves (Rushton and Somssich, 1998; Eulgem *et al*, 2000). Direct transcriptional targets have been suggested for several WRKY factors (Robatzek and Somssich, 2002), but demonstrated only for parsley *Pc*WRKY1 (Turck *et al*, 2004). WRKY proteins have also been linked to MAP kinase (MAPK) cascades in *Arabidopsis*: WRKY22 and WRKY29 are thought to function downstream of the flagellin receptor FLS2 in a pathway that includes the MAP kinase components MEKK1, MKK4/MKK5 and MPK3/MPK6 (Asai *et al*, 2002). However, molecular evidence directly linking an MAP kinase to a WRKY factor and its target gene(s) has not been reported.

MPK4 has been proposed to function in a cascade(s) that includes the MAP kinase kinases MKK1 and MKK2 and the MAPK triple kinase MEKK1 (Ichimura *et al*, 1998). Abiotic stresses and the bacterial elicitors flagellin and harpin activate MPK4 (Teige *et al*, 2004; Suarez-Rodriguez *et al*, 2007). These results appear in contrast to other reports indicating that MPK4 functions as a negative regulator of defence

responses. For example, loss-of-function *mpk4* mutants have elevated levels of the hormone salicylic acid (SA), accumulate pathogenesis-related transcripts, and have increased resistance towards biotrophic pathogens, including *Pseudomonas syringae* and *Hyaloperonospora parasitica*, but increased susceptibility towards the necrotrophic pathogen *Alternaria brassicicola* (Petersen *et al*, 2000; Brodersen *et al*, 2006). Attempts to complement *mpk4* mutants with kinase-inactive forms have led to the conclusion that MPK4 activity is needed to suppress SA-dependent defence responses and supports the model that MPK4 is a negative regulator (Brodersen *et al*, 2006). Recently, MKS1 was identified as a MPK4 substrate, and analyses of transgenic plants and transcript profiling indicated that MKS1 is required for full resistance in *mpk4* mutants. Two transcription factors WRKY25 and WRKY33 interact with MKS1 in yeast, suggesting that these two WRKYs regulate gene expression downstream of MPK4 (Andreasson *et al*, 2005).

wrky33 loss-of-function mutants support normal growth of virulent *P. syringae*, but transgenic plants that overexpress WRKY33 support enhanced growth of *P. syringae* (Zheng *et al*, 2006, 2007). In addition, *wrky33* mutants exhibit enhanced susceptibility to *Botrytis cinerea* and *A. brassicicola*, whereas overexpression of *WRKY33* increases resistance to these necrotrophs (Zheng *et al*, 2006). This suggests that WRKY33 activates genes encoding proteins required to efficiently combat necrotrophic pathogens. An example of such a gene is *PHYTOALEXIN DEFICIENT3* (*PAD3*), which encodes cytochrome *P*450 monooxygenase 71B15 (Zhou *et al*, 1999). *PAD3* is required in the last step of the synthesis of the antimicrobial compound camalexin, and *pad3* mutants exhibit enhanced susceptibility to *A. brassicicola* (Thomma *et al*, 1999; Schuhegger *et al*, 2006).

We report here that MPK4 and MKS1 associate with WRKY33 *in vivo*. Infection leads to the activation of MPK4 and phosphorylation of MKS1. Subsequently, MKS1 and WRKY33 are released from MPK4, and WRKY33 is recruited to the promoter of *PAD3*. We show that *PAD3* mRNA accumulation in response to infection is greatly reduced in *wrky33* mutants, and that WRKY33 is an effector of expression from the *PAD3* promoter in reporter gene assays. We propose how MPK4 regulates *PAD3* expression through WRKY33 upon pathogen-induced activation.

Results and discussion

Putative target genes of WRKY33

To understand how MPK4 regulates gene expression, we exploited our previous findings that MPK4 and WRKY33 may function together to regulate specific immune responses. Expression profiling was performed using ATH1 GeneChips (Affymetrix) to screen for putative target genes of WRKY33. To this end, triplicate mRNA samples of *wrky33* mutants and wild-type (Col-0) plants harvested before and 24 h after treatment with the SA analogue benzothiadiazole (BTH) were compared.

To enrich for putative WRKY33 target genes, transcripts accumulating in response to BTH treatment in wild type, but not in *wrky33*, were identified (Supplementary Table S1). Only a few genes failed to accumulate properly in BTH-treated *wrky33*. Of 29 transcripts initially identified, only 4 showed dramatic differences between wild type and *wrky33*. These four included *PAD3* and *CYP71A13*, which are strongly co-regulated and both are required for the synthesis of the phytoalexin camalexin (Zhou *et al*, 1999; Schuhegger *et al*, 2006; Nafisi *et al*, 2007). In addition, *NUDT6* and a peptidyl-prolyl isomerase (PPIase) failed to accumulate in *wrky33*. The expression of *NUDT6* has been found to be dependent on the disease regulators EDS1 and PAD4 in RPM1-conditioned responses (Bartsch *et al*, 2006). PPIase, a member of the cyclophilin family, has not been linked to resistance responses previously.

To validate these WRKY33 targets, real-time PCR was performed on BTH-treated Col-0 and *wrky33*. The mRNAs of all four genes failed to accumulate normally in *wrky33* upon BTH treatment (Figure 1A). As loss of MPK4 function leads to increased levels of SA (Petersen *et al*, 2000) but WRKY33 could function downstream of MPK4, yet upstream of SA. Therefore, we decided to broaden this analysis, and confirm the expression of the co-regulated *PAD3* and *CYP71A13* genes in a more biologically relevant context. This analysis revealed that the two genes failed to accumulate to wild-type levels in *wrky33* treated with flagellin or locally infected with *Pst* DC3000 or *Pst* DC3000 expressing the *avrRpm1* effector that triggers resistance through the host resistance gene *RPM1* (Figure 1B). *PAD3* and *CYP71A13* mRNA levels peaked 2- to 4-h after flagellin treatment and in plants infected with virulent *Pst* DC3000. In wild-type plants challenged with *Pst* DC3000 *avrRpm1*, the initial increase in *PAD3* and *CYP71A13* mRNA levels was also observed, but 4 h post-infection *PAD3* and *CYP71A13* mRNA levels were five-fold higher and again, this increase was not observed for *wrky33* (Figure 1B). These results indicate that WRKY33 is required for the accumulation of *PAD3* and *CYP71A13* mRNAs in response to flagellin and bacterial pathogens in the very early stages of infection. In addition, WRKY33 also seems to be required for further enhancement of the expression of these two genes upon *R*-gene activation.

WRKY33 binds to and activates transcription from the PAD3 promoter

Genes whose expression is not induced in *wrky33* upon BTH treatment, flagellin or infection could represent direct and indirect WRKY33 targets. To examine whether *PAD3* or *CYP71A13* could be directly regulated by WRKY33, we assayed the association of WRKY33 with putative promoter regions of these genes by chromatin immunoprecipitation (ChIP). The *PAD3* promoter contains four sequences corresponding to the core and extended WRKY-binding site or W-box (TTGAC and TTGACC/T; Eulgem *et al*, 2000) at positions −1109, −1015, −555 and −388 upstream of the *PAD3* transcription start site. A primer combination that amplified an 88-bp fragment spanning the W-box at −555 could repeatedly amplify genomic DNA (P1; Supplementary Table S2). As the sonication procedure sheared the ChIP DNA to ∼500-bp fragments, this primer combination would amplify regions of the proximal promoter containing the W-boxes at −388, −555 and possibly one or both of the more 5′ upstream boxes. We therefore assayed whether genomic DNA fragments immunoprecipitated with WRKY33 could be amplified by this primer pair by real-time PCR. Interestingly, DNA sequences from the promoters of *PAD3* and *CYP71A13* were not recovered from extracts of untreated tissue (*CYP71A13* data not shown). However, the amount of *PAD3* promoter

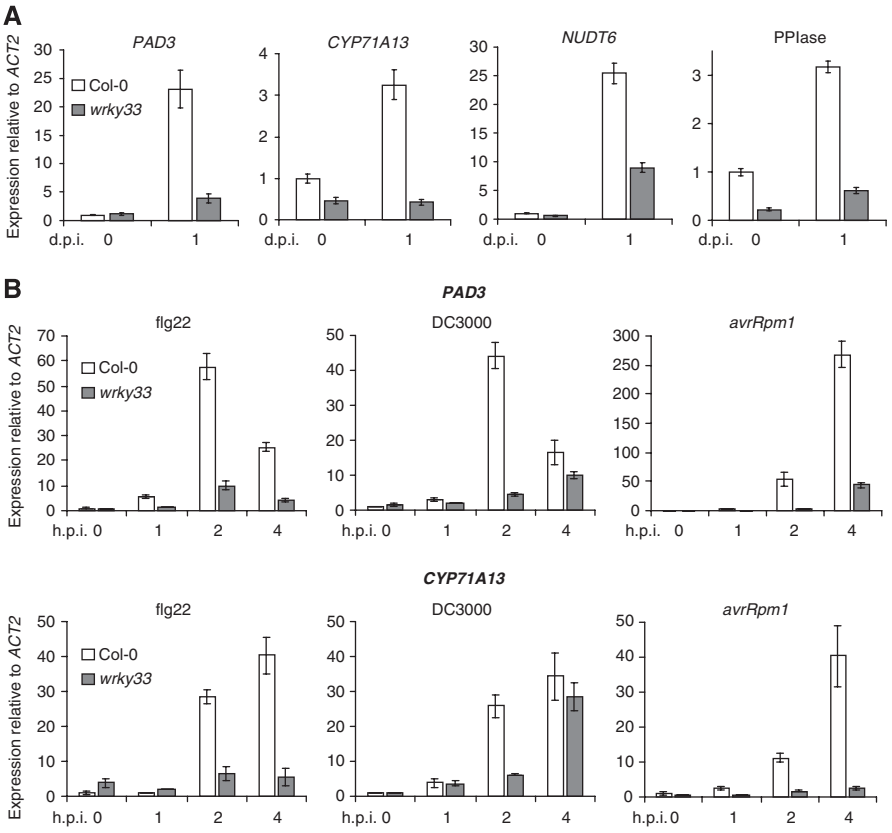

Figure 1 Real-time PCR quantitation of *PAD3*, *CYP71A13*, *NUDT6* and PPIase mRNAs. (**A**) Expression in Col-0 and *wrky33* before or 24 h after treatment with BTH. (**B**) Expression in Col-0 and *wrky33* before or after treatment with flg22, *Pst* DC3000 or *Pst* DC3000 (*avrRpm1*) for 30 min, 1, 2 and 4 h. The samples were tested in triplicate and normalized to *ACTIN2*. Means ± s.d. are shown. d.p.i.: days post-infection. h.p.i.: hours post-infection.

DNA recovered from wild-type Col-0 treated with flagellin for 1.5 and 2 h was higher than *PAD3* promoter DNA recovered from mock and *wrky33* immunoprecipitates (Figure 2A; data not shown). Next, we performed ChIP with anti-WRKY33 on wild-type Col-0 4 h post-infection with *Pst* DC3000 expressing *avrRpm1* or untreated control plants. *PAD3* promoter DNA was not amplified from DNA isolated from untreated plants, but was readily amplified from pathogen-infected plants (Figure 2B). DNA from the *PAD3* promoter was not amplified from *wrky33*-infected tissue (Figure 2B), again demonstrating the specificity of the anti-WRKY33 antibody. These results provide direct evidence that WRKY33 is recruited to the promoter of *PAD3 in vivo* in response to flagellin treatment or when plants are infected with a pathogen. In addition, it demonstrates that the presence of WRKY33 on the *PAD3* promoter correlates with the abundance of *PAD3* mRNA (Figure 1B).

To confirm the significance of WRKY33 binding to the *PAD3* promoter, we used a transient gene expression assay in leaves to monitor WRKY33-dependent gene expression from the *PAD3* promoter. Co-bombardments of a *PAD3* promoter fusion to the GUS reporter gene (*PAD3*:GUS) together with a *CaMV* 35S:*WRKY33* effector plasmid in *wrky33* mutants resulted in strong GUS activity after *Pst* DC3000 (*avrRpm1*) infection, whereas the *PAD3*:GUS construct with empty vector only resulted in very weak GUS activity (Figure 2C). As mentioned in the introduction, WRKY22 functions downstream of the flagellin receptor, FLS2, to activate early defence genes (Asai *et al*, 2002). Unlike *WRKY33*, ectopically expressed *WRKY22* did not activate *PAD3* promoter-driven *GUS* expression (Figure 2C), suggesting that *PAD3* is not a general target of pathogen-responsive WRKYs. This result demonstrates that WRKY33, and not the related WRKY22, can activate gene expression from the *PAD3* promoter upon infection.

WRKY33 is likely to regulate a number of genes other than *PAD3*. As shown above, *CYP71A13* may also be subject to regulation by WRKY33. Although initial ChIP experiments have not detected WRKY33 binding to its upstream regions, the promoter of *CYP71A13*, similar to that of *PAD3*, may well be a WRKY33 target. This is because *CYP71A13* and *PAD3* are tightly co-regulated, both are required for the synthesis of camalexin (Nafisi *et al*, 2007) and the *CYP71A13* promoter also contains a WRKY-binding site at position −286 upstream of the *CYP71A13* transcription start site. Other genes from our initial screen, such as *NUDT6*, could also represent WRKY33 target candidates downstream of MPK4. *NUDT6* expression requires WRKY33 upon infection with strains of *P. syringae* (data not shown) as well as EDS1 and PAD4, whose loss of function suppresses the *mpk4* phenotype (Bartsch *et al*, 2006; Brodersen *et al*, 2006). It is likely that our transcript profiling detected only a subset of WRKY33 target genes as *PAD3* and *CYP71A13* were induced much more strongly by flagellin and pathogen infections than by BTH. Therefore, it may be possible to identify additional WRKY33 targets by comparing transcript profiles of flagellin-treated and untreated wild-type and *wrky33* plants. Similarly, it may be useful to compare *wrky33* and *mpk4* single mutants with the double *wrky33/*

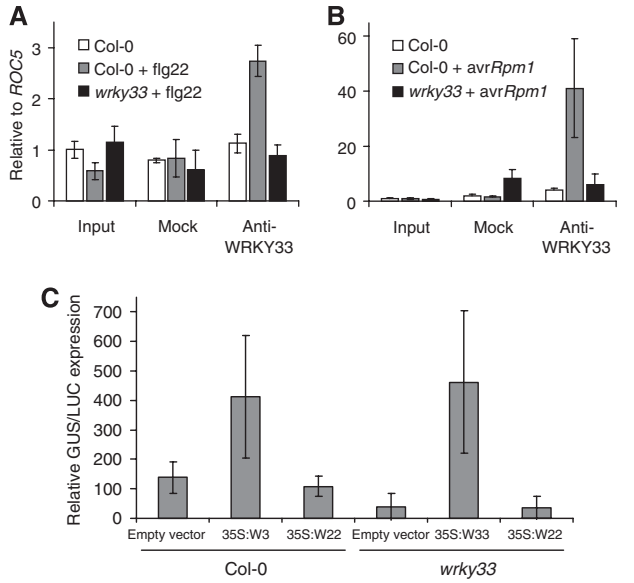

Figure 2 WRKY33 binding to and activation from the *PAD3* promoter. (**A**, **B**) Enrichment of P1 amplicons from chromatin immunoprecipitates with anti-WRKY33 antibodies from regions of the *PAD3* promoter over background (measured with primers to a promoter region of the *ROC5* control gene) in Col-0 and *wrky33* treated with flg22 for 1.5 h (A) and after treatment with *Pst* DC3000 (*avrRpm1*) for 4 h (B). The samples were tested in triplicate and normalized to *ROC5*. Means ± s.d. are shown. (**C**) Transient expression assays using a 2.4-kb fragment of the *PAD3* promoter fused to the *GUS* reporter gene (*PAD3*:GUS) inoculated with *Pst* DC3000 (*avrRpm1*). Bombardments of detached leaves of Col-0 and *wrky33* mutant were done with *PAD3*:GUS in combination with an empty vector or an effector of the *CaMV* 35S promoter driving *WRKY33* or *WRKY22* full-length cDNA. A 35S:LUC construct was used as a control for the efficiency of transient transformation. GUS activity in each sample was expressed relative to LUC activity to normalize data for variation in transformation efficiency.

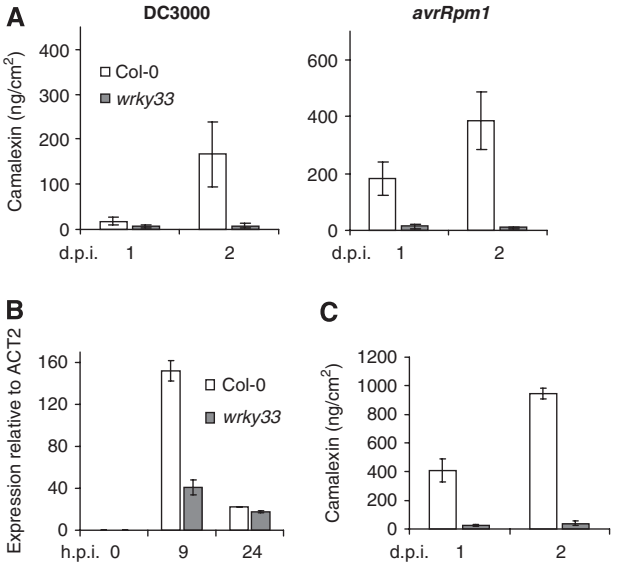

Figure 3 Levels of *PAD3* mRNA and camalexin in Col-0 and *wrky33* plants after infection with pathogens. (**A**) Camalexin levels after inoculation with *Pst* DC3000 or *Pst* DC3000 (*avrRpm1*). (**B**) Real-time PCR detection of *PAD3* mRNA after inoculation with *A. brassicicola*. The samples were tested in triplicate and normalized to *ACTIN2*. (**C**) Camalexin levels after inoculation with *A. brassicicola*. Means ± s.d. are shown. d.p.i.: days post-infection. h.p.i.: hours post-infection.

mpk4 mutant (below) to identify targets directly regulated by WRKY33 through the MPK4 pathway.

WRKY33 is required for camalexin synthesis after pathogen attack

To study the role of WRKY33 in the control of camalexin production, camalexin levels were determined in Col-0 and *wrky33* mutant plants 24 and 48 h after infection with *Pst* DC3000 or *Pst* DC3000 expressing *avrRpm1*. This showed that these pathogens induce the production of camalexin in Col-0 but not in *wrky33* mutants (Figure 3A). However, the camalexin-deficient mutant *pad3* does not exhibit altered susceptibility to these pathogens (Glazebrook and Ausubel, 1994), but is markedly more susceptible to infection by the necrotrophic fungus *A. brassicicola* (Thomma *et al*, 1999) that elicits synthesis of camalexin in *Arabidopsis* (Nafisi *et al*, 2007). We therefore used this pathogen to examine the role of WRKY33 in disease resistance. First, *PAD3* mRNA levels were determined in Col-0 and *wrky33* mutant plants 24 h after infection with *A. brassicicola* (Figure 3B); *PAD3* expression was strongly induced in wild-type but not *wrky33* plants. Similar results were obtained for *CYP71A13* (Supplementary Figure S1). The effect of reduced *PAD3* and *CYP71A13* expression on camalexin synthesis after infection was assessed by camalexin measurements. After infection with *A. brassicicola*, camalexin levels in *wrky33* plants were much lower than in wild type (Figure 3C). Thus, the disease phenotypes of *wrky33* mutants after *A. brassicicola* infection were similar to those of *pad3* (Supplementary Figure S2). Taken together, these results indicate that WRKY33 controls the production of camalexin in response to infection by activating expression of genes encoding camalexin biosynthetic enzymes.

WRKY33 is released from complexes with MPK4 upon infection

We previously showed that WRKY33 interacts in yeast and *in vitro* with the MPK4 substrate MKS1 (Andreasson *et al*, 2005). To extend these findings *in vivo*, the presence of WRKY33 was demonstrated in immunoprecipitates from nuclear extracts using an anti-MKS1 antibody (Figure 4A, top). The specificity of the MKS1 pull-down was confirmed by the absence of WRKY33 in immunoprecipitates from an *mks1* loss-of-function mutant. This *mks1* transposon insertion line (GT.108403) fails to accumulate MKS1 mRNA or protein (data not shown). Nuclear extracts were used for co-immunoprecipitation because WRKY33 and MKS1 protein levels are very low in total cellular protein extracts and because both proteins are nuclear-localized (Andreasson *et al*, 2005; Zheng *et al*, 2006). In a reciprocal experiment, MKS1 was detected in immunoprecipitates prepared using an anti-WRKY33 antibody (Figure 4A, bottom). The specificity of the WRKY33 pull-down was confirmed by the absence of MKS1 in immunoprecipitates from the *wrky33* loss-of-function mutant. These results demonstrate that WRKY33 and MKS1 interact *in vivo*, and are consistent with our earlier demonstration that MKS1 and MPK4 also interact *in vivo* (Andreasson *et al*, 2005).

To functionally link MPK4 to WRKY33, we examined whether MPK4 is found in complexes with WRKY33 *in vivo* by assaying for the presence of MPK4 in anti-WRKY33 immunoprecipitates from nuclear extracts. Interestingly,

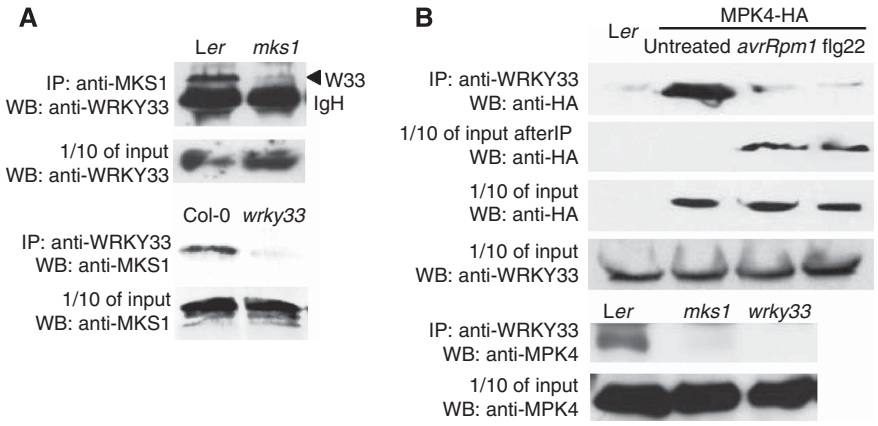

Figure 4 Complexes between WRKY33, MKS1 and MPK4. (**A**) Co-immunoprecipitation of WRKY33 and MKS1 from nuclear extracts from: Bottom, Col-0 and *wrky33* mutant immunoprecipitated with anti-WRKY33 and stained (WB) with anti-MKS1; Top, L*er* and *mks1* mutant immunoprecipitated with anti-MKS1 and stained with anti-WRKY33. One-tenth of inputs was stained with the same antibodies as a loading control. IgH: Ig heavy chain. (**B**) Top, co-immunoprecipitation of WRKY33 and MPK4 before and after treatment of *Pst* DC3000 (*avrRpm1*). Nuclear extracts of transgenic plants expressing MPK4-HA in the *mpk4* background were immunoprecipitated with anti-WRKY33 and stained with anti-HA. Wild-type L*er* plants were used as a negative control. One-tenth of input before and after the immunoprecipitation was stained with anti-HA as a control. Infected samples were harvested after 4 h. Bottom, co-immunoprecipitation performed as above for WRKY33 and MPK4 in L*er*, *mks1* and *wrky33*.

MPK4 was readily detected in anti-WRKY33 immunoprecipitates from uninfected leaves (Figure 4B). In contrast, MPK4 was barely detectable in anti-WRKY33 immunoprecipitates from leaves treated with flagellin or infected with *Pst* DC3000 expressing *avrRpm1* (Figure 4B, top). This was apparently not due to a reduction in the levels of MPK4 protein in nuclei, as MPK4 was readily detected in the supernatant of these induced extracts following immunoprecipitation of WRKY33 (Figure 4B, second panel). MPK4 and WRKY33 do not interact in yeast (Andreasson *et al*, 2005). This could imply that MPK4 and WRKY33 exist in a complex that depends on MKS1. Thus, we looked for the presence of an MPK4–WRKY33 complex in the *mks1* mutant. This showed that MKS1 is indeed required for such a complex, as we were repeatedly unable to pull down MPK4 with anti-WRKY33 in *mks1* plants (Figure 4B, bottom). Therefore, it is most likely that MKS1 forms a ternary complex with MPK4 and WRKY33 and that such complexes might sequester or regulate WRKY33.

MKS1 is needed to fine-tune PAD3 expression

The release of WRKY33 from MPK4 and/or MKS1 could be mediated by changes in the activity of MPK4 followed by phosphorylation of MKS1. PAMPs such as flagellin and virulent *Pst* DC3000 activate MPK4 (Brader *et al*, 2007; Suarez-Rodriguez *et al*, 2007). Infections with both *Pst* DC3000 and *Pst* DC3000 expressing the *avrRpm1* effector dramatically increased MPK4 activity (Figure 5A). In addition, infection with type III secretion-defective and coronatine-deficient *Pst* DC3118 COR$^-$ *hrpS*, which cannot deliver effectors into the host, lead to strong and sustained MPK4 activity (Figure 5A). Collectively, these data support a model in which MPK4 is activated by PAMPs. In addition, effectors delivered by the pathogens do not significantly contribute to MPK4 activation, indicating that MPK4 is primarily engaged in PAMP-induced defence responses.

Next, we examined the phosphorylation status of MKS1. Two MKS1 forms are detectable by SDS–PAGE; the unphosphorylated form with a higher mobility predominates in uninduced plants (Figure 5B). Infections with *Pst* DC3000 expressing *avrRpm1* or treatments with flagellin converted a portion of the faster migrating form of MKS1 into a lower mobility form caused by phosphorylation (Figure 5B; Supplementary Figure S3A). This suggests that activation of MPK4 followed by phosphorylation of MKS1 leads to the release of WRKY33 from complexes with MPK4 upon infection. To examine whether MKS1 remains in a complex with WRKY33 after its release from MPK4, we co-precipitated MKS1 with anti-WRKY33 after infection. Interestingly, MKS1 was detected in the immunoprecipitates both before and after infection (Figure 5C). Furthermore, MKS1 was not detectable in the supernatants of these extracts following immunoprecipitation, suggesting that MKS1 mostly exists in complexes with WRKY33 (Figure 5C). This assumption is supported by our inability to detect MPK4–MKS1 complexes after flagellin treatment (Supplementary Figure S3B). That MKS1 and WRKY33 are associated in plants both before and after infections suggest the MKS1–WRKY33 complex exists independently of MKS1 phosphorylation. This conclusion is supported by a pull-down experiment demonstrating the existence of MKS1–WRKY33 complexes both before and after phosphatase treatments (Supplementary Figure S3C), and that phospho-mimics, non-phosphorylatable and wild-type forms of MKS1 bind WRKY33 equally well in yeast (see Supplementary data, and data not shown). Interestingly, MPK4 also interacts equally well with these forms of MKS1 in yeast (data not shown). One model to explain this observation could be that other, as-yet unidentified factor(s) bind the MKS1–WRKY33 complex when MKS1 becomes phosphorylated facilitating MPK4 release. Nevertheless, to test the relevance of a MKS1–WRKY33 complex for WRKY33 function, we examined whether MKS1 is required for the full pathogen-induced expression of *PAD3*. As seen in Figure 5D, the accumulation of *PAD3* mRNA is lower in the early stages and higher at later stages of infection in *mks1* mutants compared with wild type. This suggests that although WRKY33 continues to activate the expression of *PAD3*, a binary complex between MKS1 and WRKY33 may optimize

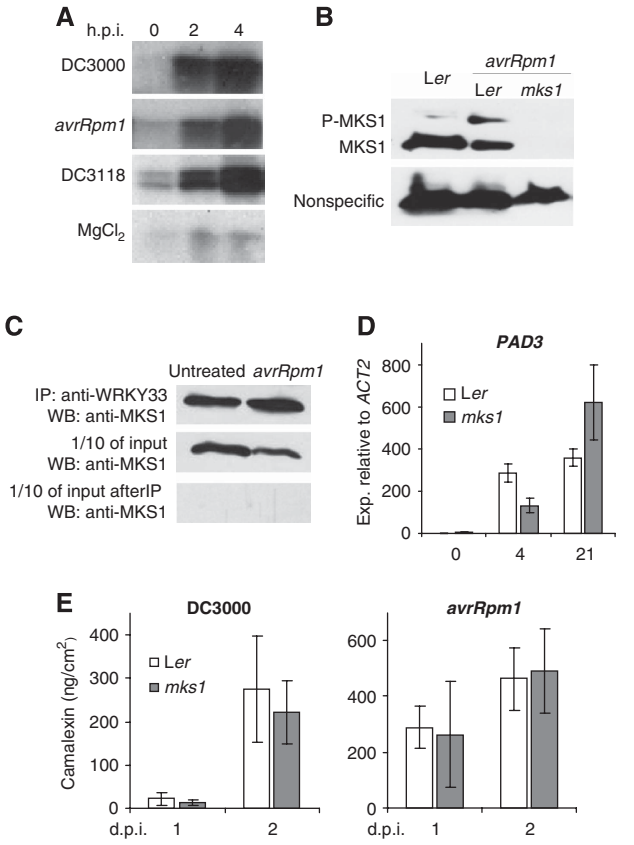

Figure 5 Effects of infection on MPK4 activity and MKS1 protein, and of *mks1* mutation on *PAD3* mRNA levels. (**A**) Kinase activity of HA-tagged MPK4 immunoprecipitated from total protein extracts was assayed using ^{32}P-labelled ATP and myelin basic protein (MBP) as substrate. h.p.i., hours post-infection. (**B**) Plants were treated with *Pst* DC3000 (*avrRpm1*) for 4 h. Total nuclear extracts in the presence of 10 μM MG-132 were resolved on 12% SDS–PAGE, blotted and stained with anti-MKS1. Nonspecific band was used as a loading control. (**C**) Co-immunoprecipitation of MKS1 and WRKY33 4 h after *P. syringae* treatments. Nuclear extracts from untreated L*er* and plants treated with *Pst* DC3000 (*avrRpm1*) were immunoprecipitated with anti-WRKY33 and stained with anti-MKS1. (**D**) Real-time PCR quantitation of *PAD3* mRNA in L*er* and *mks1* mutant before or after treatment with *Pst* DC3000 (*avrRpm1*) for 4 and 21 h. (**E**) Camalexin levels after inoculation with *Pst* DC3000 or *Pst* DC3000 (*avrRpm1*).

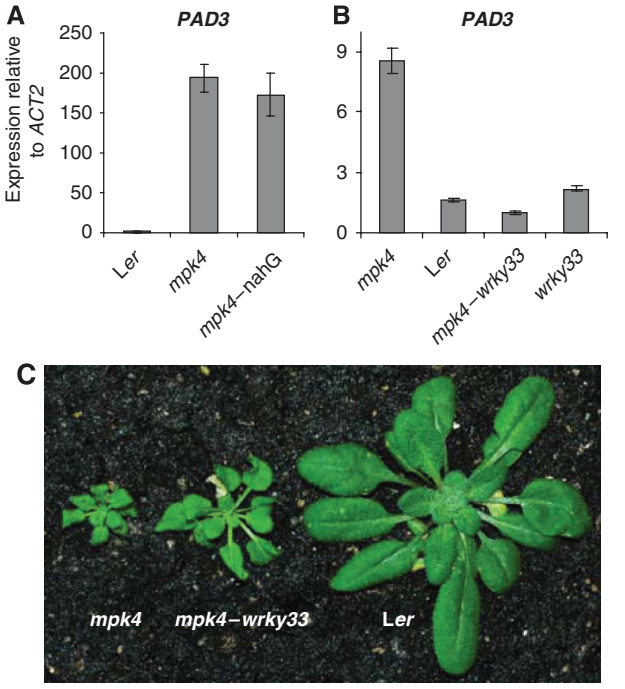

Figure 6 WRKY33 functions downstream of MPK4. (**A**) Expression of *PAD3* in L*er*, *mpk4* and *mpk4–nahG*. (**B**) Effect of *wrky33* mutation on constitutive *PAD3* expression in *mpk4*. Samples were tested in triplicate and normalized to *ACTIN2*. Means ± s.d. are shown. (**C**) Partial rescue of the *mpk4* dwarf phenotype by *wrky33* mutation.

this WRKY33 function. In this context, we note that the altered expression of *PAD3* in *mks1* mutants is insufficient to affect camalexin production (Figure 5E).

PAD3 expression in mpk4 requires WRKY33 but not SA

A large number of defence-related genes, including *PAD3*, are constitutively expressed in *mpk4* loss-of-function mutants. If WRKY33 functions directly downstream of MPK4, *PAD3* should be expressed to comparable levels in *mpk4* and in *mpk4* SA-deficient backgrounds. To this end, we compared the levels of *PAD3* in *mpk4* and *mpk4* transgenic plants expressing the SA hydroxylase *NahG*. This analysis revealed that *PAD3* is de-repressed in *mpk4* independently of SA (Figure 6A). Nonetheless, the elevation of *PAD3* mRNA in *mpk4* and *mpk4–NahG* is insufficient to result in a detectable increase in camalexin levels (data not shown), indicating that MPK4-independent factor(s) are also required to produce camalexin (Ren *et al*, 2008). To extend this analysis, we introduced the loss-of-function *wrky33* allele into the *mpk4* mutant, and confirmed double mutant progeny using PCR (data not shown). In contrast to *mpk4* single mutants that accumulate *PAD3* to higher levels than wild type, double homozygous *mpk4–wrky33* plants did not (Figure 6B). On the other hand, the *wrky33* mutation did not significantly change the accumulation of *PR1* messenger in *mpk4* (data not shown). Furthermore, *wrky33* partially suppressed the *mpk4* phenotype (Figure 6C). These results provide genetic evidence that *PAD3* is a direct target regulated by WRKY33 downstream of the MPK4 pathway independently of the accumulation of SA. Because the *wrky33* mutation only partially rescued *mpk4* phenotypes, WRKY33 is presumably not the only effector downstream of MPK4.

In summary, we show here that MPK4 functions as a regulator of PAMP-induced defence responses in *Arabidopsis*. MPK4 is activated in response to PAMPs and, similar to other MAP kinases, presumably phosphorylates effector proteins that directly or indirectly regulate a spectrum of responses. More specifically, changes in MPK4 activity and phosphorylation of MKS1 on multiple sites (Caspersen *et al*, 2007), somehow triggers the release of WRKY33 from nuclear complexes with MPK4 to permit WRKY33 to activate the expression of target genes. These targets include *PAD3* whose expression leads to the production of antimicrobial camalexin. These findings may also explain the genetic evidence that MPK4 functions as a negative regulator of basal resistance. When MPK4 is absent or dysfunctional in *mpk4* mutants, WRKY33 and presumably other transcription factors are not sequestered in nuclear complexes with the kinase in the absence of pathogens. Instead, they inappropriately activate gene expression. This mode of action is different from that reported for many other

MAP kinases and their transcription factor substrates in which the latter translocate to the nucleus following phosphorylation by the kinase in the cytoplasm (Wilkinson and Millar, 1998; Djamei *et al*, 2007).

Materials and methods

Plant growth conditions and treatments

Plants were grown in chambers with 8 h light/16 h darkness at 75% RH and 22°C. The *wrky33* mutant was *wrky33-2* (GABI_324B11; Zheng *et al*, 2006). BTH (100 μM; Bion 50WG, 50% active ingredient) was sprayed onto leaves. Bacterial infections and growth assays with *Pst* DC3000 and related strains were described previously (Mackey *et al*, 2003). The plants for camalexin assay with *Pst* DC3000, *Pst* DC3000 *avrRpm1* and *A. brassiciola* were grown in chambers with 12 h light/12 h darkness at 75% RH and 22°C. The plants were syringe-inoculated with *Pst* DC3000 or *Pst* DC3000 *avrRpm1* at a dose of $OD_{600} = 0.01$ as described by Parisy *et al* (2007). For ChIP infections, seedlings were vacuum infiltrated with *Pst* DC3000 *avrRpm1*. *A. brassicicola* infections of 3-week-old plants with strain ATCC 96866 were described previously (Nafisi *et al*, 2007). Camalexin was determined according to Glazebrook and Ausubel (1994). *Arabidopsis* plants were treated with a 10 μM flg22/0.001% Silwett solution. For ChIP, plants were grown on MS plates, transferred to liquid MS media for 24 h and flg22 was added to a final concentration of 10 μM.

RNA isolation and quantitative RT–PCR

Total RNA was extracted with Tri-Reagent RiboPure kit (Ambion, Austin, TX, USA). For quantitative PCR, RNAs were treated with RQ1 DNase (Promega, Madison, WI, USA). Quantitative RT–PCR used Superscript III Platinum SYBR Green One-Step qRT–PCR kit (Invitrogen, Carlsbad, CA, USA) with 10 pmol of each primer and 100 ng total RNA in 20 μl. Except for experiments in Figure 3 and Supplementary Figures S1 and S2, reactions were run on an icycler IQ (Bio-Rad, Hercules, CA, USA). Quantitative PCR reactions were performed in triplicate for each individual line, and quantification of threshold cycle (CT) values was achieved by calculating means of normalized expressions using Q-gene software (Muller *et al*, 2002). For Figure 3 and Supplementary Figures S1 and S2, reactions were run on an Applied Biosystems 7500 Real Time PCR. Primers for real-time PCR are in Supplementary Table S2. In all figures except Supplementary Figure S2B, qPCR result values displayed are relative to wild-type untreated plants, which are set to a relative value of 1.

Antibodies

Mouse monoclonal antibodies were against the HA epitope (clone 12CA5; Roche) and against MKS1 (HYB 330-01; Statens Serum Institut, Denmark). Rabbit polyclonal antibodies against WRKY33 peptides (CEPEAGKRWKGDNETNG and CQEQQKKNQSEQWSQT) were made by Eurogentec (Belgium). MPK4 was immunoprecipitated using anti-MPK4 (Sigma).

Western blot and kinase assays

Samples were heated for 10 min at 100°C and subjected to 12 or 15% SDS–PAGE. Electrophoresed proteins were transferred by semi-dry electrophoresis to cellulose membranes after standard protocols. Membranes were incubated with primary antibodies (1:3000) and then with horse radish peroxidase-conjugated secondary antibodies (Dako A/S, Denmark, 1:20 000) for the detection of immunoreactive bands with SuperSignal West Pico Chemiluminescent Substrate (Pierce Biotechnology, Rockford, USA). Kinase assays were performed as described previously (Brodersen *et al*, 2006).

Nuclear protein extraction and immunoprecipitation

Nuclei were isolated according to Gendrel *et al* (2002) and Nelson *et al* (2006). Nuclei were resuspended in co-immunoprecipitation buffer (100 mM Tris–Cl, 75 mM NaCl, 1 mM EDTA, 0.1% Triton X-100, 0.05% SDS, 10% glycerol, 2.5 mM DTT, proteinase and phosphatase inhibitors), and sonicated. Benzonase (10 U) was added and samples were then incubated on ice for 1 h, and centrifuged at 16 000 *g* for 30 min. The supernatants were incubated with antibodies overnight at 4°C followed by precipitation with protein A–Sepharose CL-4B or protein G-agarose beads (GE Healthcare) for 2 h. After washing four times with co-immunoprecipitation buffer, proteins were eluted by boiling in 40 μl Laemmli loading buffer for 10 min. The samples were then processed by western blotting.

ChIP

Leaves of 3- to 4-week-old wild-type (Col-0) and *wrky33* plants grown in soil, or on MS plates were vacuum-infiltrated with formaldehyde crosslinking solution and ChIP performed as described (Gendrel *et al*, 2002; Johnson and Bresnick, 2002). Samples were sonicated (Virsonic 600; Virtis) 6×10 s pulses at level 3, with 10-s breaks. Real-time PCR was used to quantify the immunoprecipitated DNA, and the quantity of *PAD3* promoter normalized to nonspecific DNA levels (ROC5 promoter; Chou and Gasser, 1997). Primers for real-time PCR are in Supplementary Table S2.

Transient gene expression assay

The 2424 bp 5′ upstream region of *PAD3* was amplified by PCR and introduced in the *Bam*HI and *Nco*I sites of a GUS reporter construct (Raventos *et al*, 1998). For the *CaMV* 35S-driven *WRKY33* or *WRKY22* constructs, *WRKY33* or *WRKY22* was PCR amplified and introduced into the *Bam*HI and *Stu*I sites of p35SE9 (Andreasson *et al*, 2005).

Leaves from 3- to 4-week-old, short-day grown wild-type or *wrky33* plants were bombarded 1–2 h after detachment as previously described (Leah *et al*, 1994). Each bombardment used ~1 mg of 1 μm gold particles coated with 1 μg of *PAD3-1*:GUS reporter, 1 μg of empty vector or WRKY33 or WRKY22 effector, and 1 μg of 35S:LUC reference plasmids. LUC expression was used to normalize transfection efficiency. Bombardments were at 2 bar with a distance of 10 cm using a Particle Inflow Gun. Bombarded leaves were incubated for about 23 h under long-day conditions, vacuum infiltrated with *Pst* DC3000 (*avrRpm1*) at 1×10^5 c.f.u./ml and incubated for another hour. The GUS activity in each sample was expressed relative to LUC activity to normalize data for variation in transformation efficiency according to Leah *et al* (1994) using a Wallac Victor II fluorometer.

Supplementary data

Supplementary data are available at *The EMBO Journal* Online (http://www.embojournal.org).

Acknowledgements

We thank Suksawad Vongvisuttikun for technical assistance. This study was supported by the Danish Research Councils to MP (23020101) and JM, (23030076, 272050367 and 272060049), and by the US Department of Energy to JG (DE-FG02-05ER15670).

References

Andreasson E, Jenkins T, Brodersen P, Thorgrimsen S, Petersen NH, Zhu S, Qiu JL, Micheelsen P, Rocher A, Petersen M, Newman MA, Bjorn Nielsen H, Hirt H, Somssich I, Mattsson O, Mundy J (2005) The MAP kinase substrate MKS1 is a regulator of plant defense responses. *EMBO J* **24:** 2579–2589

Asai T, Tena G, Plotnikova J, Willmann MR, Chiu WL, Gomez-Gomez L, Boller T, Ausubel FM, Sheen J (2002) MAP kinase signalling cascade in *Arabidopsis* innate immunity. *Nature* **415:** 977–983

Bartsch M, Gobbato E, Bednarek P, Debey S, Schultze JL, Bautor J, Parker JE (2006) Salicylic acid-independent ENHANCED DISEASE SUSCEPTIBILITY1 signaling in *Arabidopsis* immunity and cell death is regulated by the monooxygenase FMO1 and the Nudix hydrolase NUDT7. *Plant Cell* **18:** 1038–1051

Brader G, Djamei A, Teige M, Palva ET, Hirt H (2007) The MAP kinase kinase MKK2 affects disease resistance in *Arabidopsis*. *Mol Plant Microbe Interact* **20:** 589–596

Brodersen P, Petersen M, Bjorn Nielsen H, Zhu S, Newman MA, Shokat KM, Rietz S, Parker J, Mundy J (2006) *Arabidopsis* MAP kinase 4 regulates salicylic acid- and jasmonic acid/ethylene-dependent responses via EDS1 and PAD4. *Plant J* **47:** 532–546

Caspersen MB, Qiu JL, Zhang X, Andreasson E, Naested H, Mundy J, Svensson B (2007) Phosphorylation sites of *Arabidopsis* MAP kinase substrate 1 (MKS1). *Biochim Biophys Acta* **1774:** 1156–1163

Chou IT, Gasser CS (1997) Characterization of the cyclophilin gene family of *Arabidopsis thaliana* and phylogenetic analysis of known cyclophilin proteins. *Plant Mol Biol* **35:** 873–892

Couillault C, Pujol N, Reboul J, Sabatier L, Guichou JF, Kohara Y, Ewbank JJ (2004) TLR-independent control of innate immunity in *Caenorhabditis elegans* by the TIR domain adaptor protein TIR-1, an ortholog of human SARM. *Nat Immunol* **5:** 488–494

DeYoung BJ, Innes RW (2006) Plant NBS-LRR proteins in pathogen sensing and host defense. *Nat Immunol* **7:** 1243–1249

Diamond G, Kaiser V, Rhodes J, Russell JP, Bevins CL (2000) Transcriptional regulation of beta-defensin gene expression in tracheal epithelial cells. *Infect Immun* **68:** 113–119

Djamei A, Pitzschke A, Nakagami H, Rajh I, Hirt H (2007) Trojan horse strategy in *Agrobacterium* transformation: abusing MAPK defense signaling. *Science* **318:** 453–456

Eulgem T, Rushton PJ, Robatzek S, Somssich IE (2000) The WRKY superfamily of plant transcription factors. *Trends Plant Sci* **5:** 199–206

Fehlbaum P, Bulet P, Michaut L, Lagueux M, Broekaert WF, Hetru C, Hoffmann JA (1994) Insect immunity. Septic injury of *Drosophila* induces the synthesis of a potent antifungal peptide with sequence homology to plant antifungal peptides. *J Biol Chem* **269:** 33159–33163

Gendrel AV, Lippman Z, Yordan C, Colot V, Martienssen RA (2002) Dependence of heterochromatic histone H3 methylation patterns on the *Arabidopsis* gene DDM1. *Science* **297:** 1871–1873

Glazebrook J, Ausubel FM (1994) Isolation of phytoalexin-deficient mutants of *Arabidopsis thaliana* and characterization of their interactions with bacterial pathogens. *Proc Natl Acad Sci USA* **91:** 8955–8959

Ichimura K, Mizoguchi T, Irie K, Morris P, Giraudat J, Matsumoto K, Shinozaki K (1998) Isolation of ATMEKK1 (a MAP kinase kinase kinase)-interacting proteins and analysis of a MAP kinase cascade in *Arabidopsis*. *Biochem Biophys Res Commun* **253:** 532–543

Johnson KD, Bresnick EH (2002) Dissecting long-range transcriptional mechanisms by chromatin immunoprecipitation. *Methods* **26:** 27–36

Jones JD, Dangl JL (2006) The plant immune system. *Nature* **444:** 323–329

Journot-Catalino N, Somssich IE, Roby D, Kroj T (2006) The transcription factors WRKY11 and WRKY17 act as negative regulators of basal resistance in *Arabidopsis thaliana*. *Plant Cell* **18:** 3289–3302

Leah R, Skriver K, Knudsen S, Ruud-Hansen J, Raikhel NV, Mundy J (1994) Identification of an enhancer/silencer sequence directing the aleurone-specific expression of a barley chitinase gene. *Plant J* **6:** 579–589

Mackey D, Belkhadir Y, Alonso JM, Ecker JR, Dangl JL (2003) *Arabidopsis* RIN4 is a target of the type III virulence effector AvrRpt2 and modulates RPS2-mediated resistance. *Cell* **112:** 379–389

Meng X, Khanuja BS, Ip YT (1999) Toll receptor-mediated *Drosophila* immune response requires Dif, an NF-kappaB factor. *Genes Dev* **13:** 792–797

Menke FL, van Pelt JA, Pieterse CM, Klessig DF (2004) Silencing of the mitogen-activated protein kinase MPK6 compromises disease resistance in *Arabidopsis*. *Plant Cell* **16:** 897–907

Muller PY, Janovjak H, Miserez AR, Dobbie Z (2002) Processing of gene expression data generated by quantitative real-time RT–PCR. *Biotechniques* **32:** 1372–1374, 1376, 1378–1379

Nafisi M, Goregaoker S, Botanga CJ, Glawischnig E, Olsen CE, Halkier BA, Glazebrook J (2007) *Arabidopsis* cytochrome *P*450 monooxygenase 71A13 catalyzes the conversion of indole-3-acetaldoxime in camalexin synthesis. *Plant Cell* **19:** 2039–2052

Nelson JD, Denisenko O, Sova P, Bomsztyk K (2006) Fast chromatin immunoprecipitation assay. *Nucleic Acids Res* **34:** e2

Nimchuk Z, Eulgem T, Holt III BF, Dangl JL (2003) Recognition and response in the plant immune system. *Annu Rev Genet* **37:** 579–609

Parisy V, Poinssot B, Owsianowski L, Buchala A, Glazebrook J, Mauch F (2007) Identification of PAD2 as a gamma-glutamylcysteine synthetase highlights the importance of glutathione in disease resistance of Arabidopsis. *Plant J* **49:** 159–172

Petersen M, Brodersen P, Naested H, Andreasson E, Lindhart U, Johansen B, Nielsen HB, Lacy M, Austin MJ, Parker JE, Sharma SB, Klessig DF, Martienssen R, Mattsson O, Jensen AB, Mundy J (2000) *Arabidopsis* map kinase 4 negatively regulates systemic acquired resistance. *Cell* **103:** 1111–1120

Raventos D, Skriver K, Schlein M, Karnahl K, Rogers SW, Rogers JC, Mundy J (1998) HRT, a novel zinc finger, transcriptional repressor from barley. *J Biol Chem* **273:** 23313–23320

Ren D, Liu Y, Yang KY, Han L, Mao G, Glazebrook J, Zhang S (2008) A fungal-responsive MAPK cascade regulates phytoalexin biosynthesis in *Arabidopsis*. *Proc Natl Acad Sci USA* **105:** 5638–5643

Robatzek S, Somssich IE (2002) Targets of AtWRKY6 regulation during plant senescence and pathogen defense. *Genes Dev* **16:** 1139–1149

Rushton PJ, Somssich IE (1998) Transcriptional control of plant genes responsive to pathogens. *Curr Opin Plant Biol* **1:** 311–315

Schonwetter BS, Stolzenberg ED, Zasloff MA (1995) Epithelial antibiotics induced at sites of inflammation. *Science* **267:** 1645–1648

Schuhegger R, Nafisi M, Mansourova M, Petersen BL, Olsen CE, Svatos A, Halkier BA, Glawischnig E (2006) CYP71B15 (*PAD3*) catalyzes the final step in camalexin biosynthesis. *Plant Physiol* **141:** 1248–1254

Suarez-Rodriguez MC, Adams-Phillips L, Liu Y, Wang H, Su SH, Jester PJ, Zhang S, Bent AF, Krysan PJ (2007) MEKK1 is required for flg22-induced MPK4 activation in *Arabidopsis* plants. *Plant Physiol* **143:** 661–669

Teige M, Scheikl E, Eulgem T, Doczi R, Ichimura K, Shinozaki K, Dangl JL, Hirt H (2004) The MKK2 pathway mediates cold and salt stress signaling in *Arabidopsis*. *Mol Cell* **15:** 141–152

Thomma BP, Nelissen I, Eggermont K, Broekaert WF (1999) Deficiency in phytoalexin production causes enhanced susceptibility of *Arabidopsis thaliana* to the fungus *Alternaria brassicicola*. *Plant J* **19:** 163–171

Turck F, Zhou A, Somssich IE (2004) Stimulus-dependent, promoter-specific binding of transcription factor WRKY1 to its native promoter and the defense-related gene PcPR1-1 in parsley. *Plant Cell* **16:** 2573–2585

Wilkinson MG, Millar JB (1998) SAPKs and transcription factors do the nucleocytoplasmic tango. *Genes Dev* **12:** 1391–1397

Xu X, Chen C, Fan B, Chen Z (2006) Physical and functional interactions between pathogen-induced *Arabidopsis* WRKY18, WRKY40, and WRKY60 transcription factors. *Plant Cell* **18:** 1310–1326

Zheng Z, Mosher SL, Fan B, Klessig DF, Chen Z (2007) Functional analysis of *Arabidopsis* WRKY25 transcription factor in plant defense against *Pseudomonas syringae*. *BMC Plant Biol* **7:** 2

Zheng Z, Qamar SA, Chen Z, Mengiste T (2006) *Arabidopsis* WRKY33 transcription factor is required for resistance to necrotrophic fungal pathogens. *Plant J* **48:** 592–605

Zhou N, Tootle TL, Glazebrook J (1999) *Arabidopsis PAD3*, a gene required for camalexin biosynthesis, encodes a putative cytochrome *P*450 monooxygenase. *Plant Cell* **11:** 2419–2428